Estimating the concentrations of pigments and binders in lead-based paints using FT-Raman spectroscopy and principal-component analysis

Anuradha Pallipurath[1], Róza Villő Vőfély[1], Jonathan Skelton[1,2], Paola Ricciardi[3], Spike Bucklow[4] and Stephen Elliott[1*]

[1] *Department of Chemistry, University of Cambridge, Lensfield Road, Cambridge, CB2 1EW, UK*
[2]*Present address: Department of Chemistry, University of Bath, Claverton Down, Bath, BA2 7AY, UK*
[3]*Fitzwilliam Museum, University of Cambridge, Trumpington Street, Cambridge, CB2 1RB, UK*
[4]*Hamilton-Kerr Institute, University of Cambridge, Mill Lane, Whittlesford, Cambridge, CB22 4NE, UK*
**To whom correspondence should be addressed; e-mail:* sre1@cam.ac.uk.

Abstract

Understanding the composition of the paints used on works of art is crucial in attributing them to the artist or workshop which created them, as well as to devising strategies for their preservation and restoration. Much current research is focussed on the development of non-invasive spectroscopic methods, enabling *in situ* paint analysis without the need for sampling. However, while a lot of work has been done on looking at the composition of artists' materials qualitatively, little has been done to analyse them quantitatively. In this work, we investigate the use of Fourier-transform (FT) Raman spectroscopy, in isolation and in conjunction with complementary fiber-optic reflectance spectroscopy, to look at the spectral changes which occur with varying the paint/binder ratio in model historic lead-based paints. When used in conjunction with multivariate analysis, we demonstrate that it can be possible to obtain a semi-quantitative estimation of the composition of a paint film from its FT-Raman spectrum, given a set of suitable reference spectra recorded from paints produced within the workable mixture range. This represents a tentative first step towards a semi-automated and quantitative method for analysing cultural-heritage objects, which may help boost our understanding of their history, and enable conservators to make more informed decisions so as to ensure their preservation.

Keywords: FT-Raman spectroscopy, fiber-optic reflectance spectroscopy, lead-based paints, pigment-binder concentration, principal-component analysis

Introduction

Characterising the palette used to produce painted works of art can help in attributing them to specific artists or their workshops. Since each artist's studio prepared their own paints, determining their composition, i.e. the pigments and binding materials used to make them, as well as the ratio of the components, can be instrumental in such attributions.

Non-invasive spectroscopic identification of both the pigments and binders in painted layers is fast becoming the norm, as the methods are not only quick and relatively easy to interpret, but, crucially, do not require the removal of samples. Infra-red[1], Raman[2-10], X-ray fluorescence[2,3,11,12] and fiber-optic reflectance (FORS)[3,13-17] spectroscopies are all widely used for the analysis of cultural-heritage objects, and all four techniques can be applied *in situ*, using portable instrumentation, and without sampling. In contrast, although techniques like GC-MS[18-21] and HPLC[22-24] have been used to obtain quantitative insight into the composition of paint binders, e.g. by obtaining the ratios of different fatty acids or amino acids present in them, they invariably do require sampling, and thus are not always viable analytical techniques.

Although much work has been done on identifying pigments[2,6,11,25-29] and binders[21,30-39], and also understanding their ageing processes[12,40-42], relatively little has been done towards quantifying the proportions of components in paint mixtures, e.g. the ratio of pigments and binders present, through non-invasive means. Rampazzi *et al.* were the first to use partial least-squares (PLS) analysis of atomic absorption spectra to effectively estimate the binder/aggregate ratios in mortars, representing a step forward from the more traditional chemical analysis, which was both tedious and also heavily influenced by the wearing of the mortar due to acid attacks[43]**.** Csefalvayova *et al.*[44] showed that using partial least-squares regression (PLSR) analysis, in conjunction with FT-IR spectroscopy, enabled quantitative classification of the gelatin material present in historic papers. More recently, it was established that the C-H region of the IR spectrum can be used to classify paint binders, while the ester C=O region is best for quantification using PLSR techniques[45].

While qualitative analyses are sufficient for many research purposes, a study of ageing carried out by Boon *et al.*[46] found that paints prepared with higher binder-to-pigment ratios tend to undergo hydrolysis reactions more rapidly than those made with lower ratios. In light of this, it could be highly useful to have a semi-automated method, based on non-invasive analysis techniques, for quantifying pigment-binder ratios, in order to help conservators make more informed choices regarding the treatment of objects.

In this work, we have investigated the changes which occur in the FT-Raman and FORS spectra of simulated medieval paint films as a function of composition. As a method for analysing paints, FT-Raman spectroscopy using 1064 nm laser light is especially useful as, at this wavelength, fluorescence from the binding media is minimised, thereby giving better Raman-spectroscopic signals from the organic material. FORS spectra extend from the UV-visible region of the spectrum into the short-wave IR, and can provide quantitative information about colour, as well as absorption bands corresponding to vibrational overtones and combinations, which can be useful signatures of organic materials and functional groups. As explored in a previous study[39], both techniques can yield complementary information to characterise pigment-binder mixtures, which is especially useful when used with pattern-recognition techniques, such as principal-component analysis (PCA).

Building on this work, we test the utility of Raman and FORS spectroscopy with PCA as a semi-automated analytical technique to help quantify the relative amounts of pigments and binders in paint mixtures.

Experimental

Sample Preparation

Based on our previous study[39], in which we found that multivariate analysis of Raman spectra was most successful for paint films made up with lipid-based binders, we chose the lead white –egg yolk and lead tin yellow – poppy oil systems as model paints. Both of these, particularly the former, are frequently encountered on historic painted objects. The lead white (LW) pigment used in this study was prepared according to the traditional artists' method of placing lead ribbon over vinegar, which promotes the formation of lead carbonate on the surface; this was then scraped off and used to prepare paints as described below. Lead-tin yellow (LTY) was purchased from Kremer Pigments Inc. and used without any further processing. LTY exists in "light" and "dark" forms, the difference in colour between them being due to the difference in the stoichiometry with regard to tin in the former, and both forms were studied in this work. Egg yolk (EY; obtained from free-range eggs) and cold-pressed poppy oil (PO), used as binders, were both purchased locally.

Paint mixtures were prepared using criteria employed by artists, i.e. by mixing a pigment and binder until a paint with appropriate mechanical and optical properties was obtained. Paints were made by mixing pigments and binders in different proportions within the workable mixture range. LW and EY were mixed in pigment-binder wt/wt ratios of 2:1 (66.7% LW), 3:2 (60% LW), 1:1 (50% LW), 2:3 (40% LW) and 1:2 (33.3% LW), and LTY and PO in pigment percentages of 76.2%, 81.5%, 84.4%, 87.7% and 88.5% for LTY-dark, and 66.7%, 78.7%, 80%, 81.8%, 84.8%, 86.1%, 89% and 89.8% for LTY-light. We note that the workable mixture range is much smaller for the LTY-PO combination compared to the LW-EY combination, and therefore the LTY samples made had a relatively narrow difference in the wt% of the pigment and binder. The prepared paints were painted onto microscope glass slides and allowed to dry on a bench top for a month, after which they were stored in a light-tight box.

Spectroscopy

FT-Raman spectra were collected using a Bruker RAM II instrument (1064 nm wavelength, ~1 mm spot size, KBr beam splitter and Ge detector, ~2.37 mm penetration depth), and recorded within the range of 20 - 3600 cm^{-1} at a resolution of 4 cm^{-1}. 256 scans were integrated (requiring ~7 minutes per spectrum), and a laser power of 100 mW was used. FORS spectra were collected using a FieldSpec 4 spectroradiometer (ASD, Inc., USA; halogen lamp, ~3 mm spot size, 512-element Si array detector for visible and VNIR, and two InGaAs detectors for the ranges between 1000 - 1800 nm and 1800 - 2500 nm). With this instrument, a spectral resolution of 3 nm at 700 nm and 10 nm within the 1400 - 2500 nm range, with a scanning time of 100 ms, was possible.

Principal-Component Analysis

PCA was carried out as per the optimised conditions described in our previous work[39]. FT-Raman spectra were pre-processed by applying a 21-point triangle smoothing filter, followed by vector normalisation. We found that the triangle filter, with this relatively small window size, gave a good balance between removing noise from spectra while preserving the shape and intensity of spectral features; we note however that, for raw spectra which are smooth, a filtering step may not be necessary. The wavenumber axes of the spectra were adjusted to a common set of spectral bands, linearly interpolating the intensities where required, before constructing the PCA training matrix. 1000 and 1500 data points were used for PCAs in the spectral regions between 100 and 1800, and 100 and 3200 cm^{-1}, respectively. FORS spectra were vector normalised, and in the combined PCAs, the composite spectra were formed of 1000 points each of FT-Raman and FORS data.

When constructing the PCA matrix, the data were mean-centred, but, in contrast to our previous work, not standardised. When working, as in the present study, with datasets in which band intensities are the key source of variation between spectra, standardisation would effectively compress the apparent variance for spectral bands which change most with concentration, while expanding it for bands where changes are less pronounced. As standardisation was the only option in the PCA package we used, a small modification to one of the routines was required. All analysis routines were implemented in Python 3[47], using the NumPy[48], SciPy[49] and Matplotlib[50] packages.

Results and Discussion

In order to establish which spectral features may act as signatures of composition, we first studied the FT-Raman spectra of paint films made up with different pigment/binder ratios. Figure 1 shows Raman spectra of LW-EY paints, scaled to the height of the peak at 2926 cm^{-1} (C-H stretching). Increases in intensity of the carbonate peak at 1051cm^{-1} and the peaks due to the LW phonons at 62 cm^{-1} are both clearly visible. Similarly, a clear increase in the intensity of a peak at 1381 cm^{-1}, also attributed to LW[10], with LW concentration is also evident (inset). The peak at 1497 cm^{-1}, attributed to aliphatic C-C vibrations, was observed only in the spectrum of pure EY, and was not visible in spectra of the paint mixtures.

In the case of LTY, both LTY-light and LTY-dark paints were studied. FT-Raman spectra of paints made up with PO as the binder, scaled to the height of the band at 1440 cm^{-1}, are shown in Figure 2. As in the spectra of LW paints, peaks from LTY, occurring from 20 to around 600 cm^{-1}, show a noticeable increase in intensity with pigment concentration. The spectra of LTY-light paints also display prominent fluorescence from around 2000 - 3000 cm^{-1}, which becomes more noticeable with higher pigment concentrations, although the origin of the fluorescence is not clear at present. Aside from this, it can be seen that bands around 1740 cm^{-1} (C=O) and 1640 cm^{-1} (amide I) are broader in the spectrum of pure PO, in comparison with the paint mixtures, which is most noticeable in Figure 2b. In addition, the peak at 1720 cm^{-1}, and also the feature at 1657 cm^{-1} (C=C), are both relatively weak in the PO spectrum, again most noticeably when compared against the spectra of paints of LTY-dark. Peaks at 1497 cm^{-1} (CH_2 deformation) and 1242 cm^{-1} (C-H stretching) were observed in the PO spectrum, but were absent in the spectra of the paint mixtures; these extra peaks are related to the drying

of PO, and are due to the fact that this sample, prepared along with those studied in previous work[39], was older than the others.

Since there are clear trends in spectral features linked to the pigment/binder ratio in both systems, PCA of the Raman spectra of the paints was carried out. The result of this analysis for the LW-EY mixtures, using the spectral region between 100 and 1800 cm^{-1}, is shown in Figure 3. Strikingly, we found that, on a scatter plot of the first two principal components (Figure 3a), the different compositions formed bands, arranged in order of decreasing concentration. To test whether this phenomenon could be exploited to perform concentration estimation, we omitted the 1:1 (50% pigment) spectra from the training set, and subsequently projected these samples onto the plot using the training matrix. Points from these spectra formed a band roughly between the 60 and 40% samples, thus providing a reasonable estimate of the paint composition.

Loading plots for the first two PCs are shown in Figure 3b. It can be seen from these that in PC1, which explains over 90% of the variance among the spectra, the highest weights are assigned to part of the phonon band from 100 cm^{-1} upwards, as well as to the major bands between ~1200 and 1700 cm^{-1} identified in Figure 1. The loading plot for PC2 is relatively flat, with a handful of features representing regions of the spectrum where the concentration dependence is less clear; however, as PC2 explains only 6 % of the total variance, some of the features may be due to statistical noise. The negative weights assigned to the phonon bands and carbonate peaks in PC1 appear to be primarily responsible for the ordering of the bands in increasing concentration from right to left along PC1.

To investigate the effect of standardising the training data before performing the PCA, we carried out the same analysis with this pre-processing applied (the default option in the Matplotlib code[50]; see supporting information). The same band formation and ordering was observed, although the loading plots and the variance fractions explained by the first two PCs (69.7 and 21.9 %, respectively) were significantly different. Despite this, on treating the 50% composition spectra as unknowns, we found that it was still possible to use this analysis to estimate their concentration.

A similar analysis was also carried out using combinations of LTY-light/dark with PO (Figure 4). We opted to analyze both forms together, in order to ascertain whether a PCA to estimate concentration could simultaneously be used to identify the form of LTY present. For this analysis, we opted to use the spectral region between 1100 and 3200 cm^{-1}, which includes the C-H region, where fluorescence from LTY-light may enable the differentiation between the two forms of LTY (Figure 2), as well as the pigment peaks below ~600 cm^{-1}, which are similar in both pigments but strongly composition dependent.

On the score plot (Figure 4a), it is immediately striking that the LTY-dark and light spectra separate into the positive and negative PC1 halves, respectively (Figure 4a). Similarly to the LW-EY analysis, the LTY-dark spectra form a set of bands, arranged along PC2 in order of increasing pigment concentration. The LTY-light spectra form clusters on the scatter plot, with a considerable spread, although the groups of markers are again roughly ordered by composition along

The loading plot of PC1 (Figure 4b), which in this case explains 76.5% of the spectral variance, shows that the LTY-light fluorescence is assigned a large positive weight, and the region of the spectrum below 2100 cm^{-1}, particularly part of the LTY bands below 600 cm^{-1}, a negative weight. This explains the division of the

LTY-light and dark spectra into the positive and negative PC1 regions of the scatter plot. PC2 explains 21.3% of the variance, which is statistically significant, and, according to the loading plot, weighs the LTY bands and C-H peak positively and negatively, respectively. Since these peaks, certainly the former, reflect the paint composition for both forms of LTY, this explains the (rough) ordering of both sets of spectra along PC2 in increasing concentration.

LW has been reported to induce molecular-level changes to the amino acids present in EY[51] and, as well as forming lead soaps, is also known to accelerate the degradation of the binders, by interacting with them and causing the release of formic acid[52]. To confirm that such interactions were, in part, responsible for the spectral changes occurring with paint composition, we simulated model pigment-binder spectra by averaging the spectra of the pure components in the mixing proportions, and projected these onto a PCA score plot formed by analysis of the "real" spectra (this time including the 1:1 spectra in the training set; see supporting information, Figure S8). As expected, the simulated LW-EY spectra did not come close to the experimental ones, indicating that the spectra of the paint mixtures are not a combination of those of the pure components. However, LW-EY spectra simulated instead by interpolating between real spectra fell between the bands on the plot, in positions indicating their interpolated concentration. On the other hand, we found that spectra of LTY-PO paints created additively did fall within the clusters containing the experimentally-recorded ones, which suggests that the effect is not as pronounced in this system**.**

To investigate the LW-EY interaction further, thermal analyses of pure LW, pure EY and one test sample (2:1 LW:EY) were carried out. Differential scanning calorimetry (DSC) data suggested that the decomposition of pure EY and LW had onset temperatures of 93.2 °C and 242.8 °C, respectively, while the LW-EY paint exhibited several peaks at lower temperatures, which were absent in the pure components, and two major decompositions at onset temperatures of 221 °C and 287.5 °C (see supporting information, Figures S1-S3). This reinforces the notion that there is a complex interaction between LW and the binder, which is presumably a key part of the LW-EY spectra not simply being additive sums of their components. We also note that, unlike work done previously on aged LW-EY samples[25], the reactions observed here appeared to be endothermic in nature.

To test the possible application of concentration determination using the PCA method, over and above the concentration estimation illustrated in Figure 3, we attempted to quantify the compositions of several unknown samples of LW-EY and LTY-PO paints which had previously been prepared according to artists' recipes and were qualitatively labelled as being 'rich' and 'lean' in binder.

The samples of LW-EY both fell outside the bands in Figure 3 along PC2 (see supporting information, Figure S9). If it is assumed that this is not significant, the 'lean' sample could be estimated from its position along PC1 to have an LW concentration close to 50%. The projected 'rich' spectra display a large amount of scatter, but consistently fall below the 33.3% LW references along PC1, suggesting that the LW concentration in these samples falls outside the lower limit of the reference spectra used in the training set.

The apparent anomalies in the LW-EY matching could be due to various factors, including the LW composition, i.e. anhydrous (cerussite) vs. basic (hydrocerussite), layer thickness, or a different degree of ageing, possibly determining the extent of the reaction between LW and its binding medium suggested by the DSC. With regard to the first of these points, the paints used in the present study and the 'unknown' LW-EY samples were prepared from different batches of home-grown LW. Powder X-ray diffraction (PXRD) patterns of the LW used in the reference paints and of the unknown LW-EY sample were recorded and compared with PXRD patterns of cerussite and hydrocerussite generated from the structural information available in the literature[53,54] (see supporting information, Figures S4-S7). The pure LW used to make the reference paints most resembled hydrocerussite and, while it was harder to interpret the LW-EY spectrum, due to the presence of peaks from EY, it lacked the major 2θ peaks seen in basic LW. Based on this, then, the LW used to prepare the unknown sample may have been of a different composition than that used to make the reference paints, which could be why the matching of these samples worked less well than the estimation of the composition of paints prepared from the same batch of LW as the references.

Both the LTY-PO samples fell into the LTY-light half of the plot (Figure 4), with the samples 'lean' in binder clustering near the high-LTY percentage points, and those 'rich' in binder being lower than the 66.7% LTY points along PC2. This is consistent with the 'rich' and 'lean' paints having being prepared at the lower- and higher-LTY-content ends of the workable mixture range, respectively, and illustrates that, despite the scatter of the LTY-light references, at least a qualitative estimation of the composition of unknown paint samples from their FT-Raman spectra may still be possible.

For comparison, we also carried out PCAs of the dark and light LTY paints separately (see supporting information, Figures S10 and S11). As expected, the LTY-dark analysis behaved much like the LW-EY one, in that the bands were arranged in order of concentration along PC1, which explained over 90% of the variance. The LTY-light score plot displayed the same sort of scatter as is evident in Figure 4a, and the variance in this plot was split 70%/26.5% between PC1 and PC2. In both analyses, the loading plots illustrate that the key spectral features, viz. the C-H region, including the part of the spectrum in which LTY-light fluoresces, and the LTY bands, are used to explain the variance. However, we note that in these independent analyses, the unknown samples, certainly the 'lean' one, could be grouped with either form of LTY, whereas in the combined analysis, it is possible to determine unambiguously of which form it was made up.

Finally, as we established in our previous study[39], combining complementary FORS data with Raman spectra can sometimes improve PCA, leading to better separation and clustering. To test whether additional data might improve the concentration estimation, we recorded FORS spectra of the LW-EY reference paints, combined these with the Raman spectra between 100 and 1800 cm^{-1}, and performed PCA on the composite spectra. Although tighter clusters were formed by this method, the bands were no longer ordered by concentration, which suggests that these combined datasets are not as suitable for concentration estimation. Overall, this analysis suggests that Raman spectra are more sensitive to the subtle chemical changes which occur

with differences in pigment/binder ratio, although it is possible that, for some systems, combined Raman-FORS analyses could be more effective.

We close with a few final remarks regarding the general applicability of our analysis. As discussed above, FT-Raman using 1064 nm laser light represents an attractive method, since fluorescence from the binding media is minimal at this wavelength. However, portable Raman equipment often operates at shorter wavelengths (e.g. 532 nm), and it may not be possible to use long acquisition times and/or high laser powers in some situations; therefore, for *in situ* analysis, collecting spectra using different parameters may be necessary. Nonetheless, the method employed here is applicable to generic FT-Raman spectra, and indeed to other data sources. In this regard, pattern-recognition techniques like PCA potentially represent a general means to interpret spectral data, since they are able to identify variation in the presence of background noise. On the other hand, PCA is not inherently a quantitative technique, and once a particular form of spectroscopy is shown to be quantitative, other chemometric methods, such as partial least-squares, partial linear regression and multiple linear regression, or even peak-fitting, may be more suitable for some systems. The potential for concentration estimation illustrated in the present work does, however, complement the robust qualitative analysis provided by PCA. Finally, it is also important to note that paints in real artwork typically have undergone significant ageing, which is likely to lead to changes in spectral features which are not reflected in freshly-prepared reference samples. More work therefore needs to be done to validate the application of this method to aged paint films.

Conclusions

The results presented here suggest that it may be possible to use FT-Raman spectroscopy, in conjunction with multivariate analysis, to obtain reasonable estimates of the pigment/binder ratios in a paint film, given a suitable set of reference spectra from paints prepared over the range of workable mixture compositions. Although there are several *caveats* to our method, e.g. the possible inability to analyse LW samples containing substantial amounts of hydrocerussite using cerussite-based references, these findings may extend the utility of Raman-scattering measurements in cultural-heritage science, by making it possible to characterize artists' painting materials in a more quantitative sense. This work may therefore represent a tentative first step towards the development of computer-assisted methods for the *in situ*, non-invasive and quantitative analysis of painted cultural-heritage objects. However, in order to investigate its broader applicability, further validation needs to be done on other common paint mixtures (i.e. other pigments or binding media) and with other common Raman-measurement setups, as well as on the application of this method to real artwork, where the effects of aspects such as pre-processing of products, the nature of the substrate and the degree of ageing may become apparent.

Acknowledgements

AP wishes to thank St. John's College, Cambridge for a Benefactor's scholarship and the Alexander-Goetz program and ASD Inc/Panalytical for lending the FieldSpec4 spectroradiometer. JMS is indebted to

Trinity College, Cambridge, for provision of an internal graduate studentship which part-funded these studies. RVV is grateful to Trinity College, Cambridge for the provision of a Summer Studentship.

Figure Captions

Figure 1: FT-Raman spectra of paint mixtures of lead white and egg yolk mixed with different percentages of the pigment and binder. The spectra are scaled to the C-H stretching band at 2926 cm^{-1}, in order to show the changes in the spectra with concentration. Changes in the lead-white peaks between 1000 and 1600 cm^{-1} are clearly visible, as are changes in the phonon bands between 20 and 200 cm^{-1}. There is also a change in a peak at 1381 cm^{-1} (inset), which has been attributed to the pigment (Ref. 10). The peaks referred to in the text are marked with asterisks.

Figure 2: FT-Raman spectra of paints made up of light (a) and dark (b) lead-tin yellow in poppy oil. In both plots, the spectra are scaled to the band at 1440 cm^{-1}, to show the relative changes in intensity with the concentrations of the components. The peaks at 1497 cm^{-1} (CH_2 deformation) and 1242 cm^{-1} (C-H stretching) are due to the drying of the oil, and are marked by arrows on the inset plots. The peaks referred to in the text are marked with asterisks.

Figure 3: Principal-component analysis of FT-Raman spectra of a concentration series of lead white (LW)-egg yolk (EY) paints, with spectra of the 33.3%, 40%, 60% and 66.7% LW samples used in the training set. Spectra taken from different points on the same concentration sample form bands, arranged along PC1 in order of decreasing wt% of lead white. When projected onto the plot (a), spectra from the 50% samples fall roughly between the 40% and 60% bands, allowing the pigment/binder ratio in the paint to be estimated. This illustrates that, given a suitable set of reference spectra, this method could potentially be used to estimate the composition of an unknown LW-EY paint from its FT-Raman spectrum. The loading plots for the first two principal components (b), giving the weights assigned to different spectral bands, show that the features highlighted in the spectra in Figure 1 are responsible for the discrimination. Notably, PC1 explains over 90% of the variance, and, although the loading plot for PC2 shows weight being assigned to particular parts of the spectra, its explained variance of 6% could be largely statistical noise.

Figure 4: (a) Principal-component analysis of paints made up of lead-tin yellow (both light and dark) in poppy oil. (b) Loading plots for the first two principal components. In plot (a), the light and dark samples fall into the positive and negative PC1 halves of the plot, respectively. The dark LTY samples form bands, arranged in order of LTY concentration along PC2. The light LTY samples display a considerable amount of scatter between spectra taken from different points on some samples, although a rough ordering of the points by concentration along PC2 is again evident. Despite the scatter, identification of the form of LTY in unknown LTY paints (denoted by ‘x’ markers), qualitatively labelled as being ‘rich’ and ‘lean’ in binder, is possible, as is a rough estimation of their compositions - the position of the projected points along PC2 suggests the ‘rich’ and ‘lean’ samples were prepared at the low and high-LTY content ends of the workable mixture range, respectively.

References

[1] M. R. Derrick, D. Stulik, J. M. Landry, *Infrared spectroscopy in conservation science*, J. Paul Getty Trust, USA, **1999** .

[2] T. D. Chaplin, R. J. H. Clark, M. Martinon-Torres, *Journal of Molecular Structure* **2010** ; *976* , 350.

[3] L. Appolonia, D. Vaudan, V. Chatel, M. Aceto, P. Mirti, *Analytical and Bioanalytical Chemistry* **2009** ; *395* , 2005.

[4] A. Duran, M. L. Franquelo, M. A. Centeno, T. Espejo, J. L. Perez-Rodriguez, *Journal of Raman Spectroscopy* **2011** ; *42* , 48.

[5] H. G. M. Edwards, D. W. Farwell, L. Daffner, *Spectrochimica Acta Part A - Molecular and Biomolecular Spectroscopy* **1996** ; *52* , 1639.

[6] T. D. Chaplin, R. J. H. Clark, D. Jacobs, K. Jensen, G. D. Smith, *Analytical Chemistry* **2005** ; *77* , 3611.

[7] I. R. Lewis, H. Edwards, *Handbook of Raman Spectroscopy: From the Research Laboratory to the Process Line*, Marcel Dekker, Inc., USA, **2001** .

[8] M. Castanys, R. Perez-Pueyo, M. J. Soneira, E. Golobardes, A. Fornells, *Journal of Raman Spectroscopy* **2011** ; *42* , 1553.

[9] C. Miliani, F. Rosi, B. G. Brunetti, A. Sgamellotti, *Accounts of Chemical Research* **2010** ; *43* , 728.

[10] L . Burgio, R. J. H. Clark, *Spectrochimica Acta Part A - Molecular and Biomolecular Spectroscopy* **2001** ; *57* , 1491.

[11] F. Rosi, A. Burnstock, K. J. van den Berg, C. Miliani, B. G. Brunetti, A. Sgamellotti, *Spectrochimica Acta Part a - Molecular and Biomolecular Spectroscopy* **2009** ; *71* , 1655.

[12] W. Faubel, R. Simon, S. Heissler, F. Friedrich, P. G. Weidler, H. Becker, W. Schmidt, *Journal of Analytical Atomic Spectrometry* **2011** ; *26* , 942.

[13] S. Acquaviva, E. Danna, M. L. De Giorgi, A. Della Patria, L. Pezzati, *Applied Physics A - Materials Science & Processing* **2008** ; *92*, 223.

[14] M. Bacci, *Sensors and Actuators B - Chemical* **1995** ; *29*, 190.

[15] A. Casini, M. Bacci, C. Cucci, F. Lotti, S. Porcinai, M. Picollo, B. Radicati, M. Poggesi, L. Stefani, *Proceedings of the SPIE - The International Society for Optical Engineering* **2005** ; *5857*, 177.

[16] G. Dupuis, M. Elias, L. Simonot, *Applied Spectroscopy* **2002** ; *56*, 1329.

[17] M. Picollo, M. Bacci, A. Casini, F. Lotti, S. Porcinai, B. Radicati, L. Stefani, in Optical Sensors and Microsystems, (Eds: S. Martellucci, A. N. Chester, A. G. Mignani), Springer, New York, **2000**, pp. 259-265.

[18] K. Kahrim, A. Daveri, P. Rocchi, G. de Cesare, L. Cartechini, C. Miliani, B. G. Brunetti, A. Sgamellotti, *Spectrochimica Acta Part a-Molecular and Biomolecular Spectroscopy* **2009** ; *74* , 1182.

[19] I. Bonaduce, H. Brecoulaki, M. P. Colombini, A. Lluveras, V. Restivo, E. Ribechini, *Journal of Chromatography A* **2007** ; *1175* , 275.

[20] J. Blasko, R. Kubinec, B. Husova, P. Prikryl, V. Pacakova, K. Stulik, J. Hradilova, *Journal of Separation Science* **2008** ; *31* , 1067.

[21] R. Mateo-Castro, J. V. Gimeno-Adelantado, F. Bosch-Reig, A. Domenech-Carbo, M. J. Casas-Catalan, L. Osete-Cortina, J. De La Cruz-Canizares, M. T. Domenech-Carbo, *Fresenius Journal of Analytical Chemistry* **2001** ; *369* , 642.

[22] R. Zangrando, R. Piazza, W. R. L. Cairns, F. C. Izzo, A. Vianello, E. Zendri, A. Gambaro, *Analytica Chimica Acta* **2010** ; *675* , 1.

[23] J. P. Vicente, J. V. G. Adelantado, M. T. D. Carbo, R. M. Castro, F. B. Reig, *Talanta* **2004** ; *64* , 326.

[24] J. P. Vicente, J. V. G. Adelantado, M. T. D. Carbo, R. M. Castro, F. B. Reig, *Journal of chromatography A* **2005** ; *1076* , 44.

[25] N. S. Cohen, M. Odlyha, R. Campana, G. M. Foster, *Thermochimica Acta* **2000** ; *365* , 45.

[26] M. Bacci, M. Picollo, G. Trumpy, M. Tsukada, D. Kunzelman, *Journal of the American Institute for Conservation* **2007** ; *46* , 27.

[27] L. Burgio, D. A. Ciomartan, R. J. H. Clark, *Journal of Molecular Structure* **1997** ; *405* , 1.

[28] L. Burgio, R. J. H. Clark, R. R. Hark, *Proceedings of the National Academy of Sciences of the United States of America* **2010** ; *107*, 5726.

[29] L. Burgio, R. J. H. Clark, K. Theodoraki, *Spectrochimica Acta Part A - Molecular and Biomolecular Spectroscopy* **2003** ; *59* , 2371.

[30] S. Kuckova, I. Nemec, R. Hynek, J. Hradilova, T. Grygar, *Analytical and Bioanalytical Chemistry* **2005** ; *382* , 2577.

[31] P. Vandenabeele, B. Wehling, L. Moens, H. Edwards, M. De Reu, G. Van Hooydonk, *Analytica Chimica Acta* **2000** ; *407* , 261.

[32] P. G. Popescu, C. Enache-Preoteasa, F. D. Badea, *Revista De Chimie* **2012** ; *63* , 367.

[33] J. D. J. van den Berg, K. J. van den Berg, J. J. Boon, *Progress in Organic Coatings* **2001** ; *41* , 143.

[34] E. Manzano, J. Garcia-Atero, A. Dominguez-Vidal, M. J. Ayora-Canada, L. F. Capitan-Vallvey, N. Navas, *Journal of Raman Spectroscopy* **2012** ; *43* , 781.

[35] S. Dallongeville, M. Koperska, N. Garnier, G. Reille-Tailefert, C. Rolando, C. Tokarski, *Analytical Chemistry* **2011** ; *83*, 9431.

[36] I. Bonaduce, L. Carlyle, M. P. Colombini, C. Duce, C. Ferrari, E. Ribechini, P. Selleri, M. R. Tine, *Journal of Thermal Analysis and Calorimetry* **2012** ; *107* , 1055.

[37] E. Marengo, M. C. Liparota, E. Robotti, M. Bobba, *Analytica Chimica Acta* **2005** ; *553* , 111.

[38] E. Manzano, L. R. Rodriguez-Simon, N. Navas, R. Checa-Moreno, M. Romero-Gamez, L. F. Capitan-Vallvey, *Talanta* **2011** ; *84* , 1148

[39] A. Pallipurath, J. Skelton, P. Ricciardi, S. Bucklow, S. Elliott, *Journal of Raman spectroscopy* **2013** ; *44* , 866

[40] N. Salvado, S. Buti, J. Nicholson, H. Emerich, A. Labrador, T. Pradell, *Talanta* **2009** ; *79* , 419.

[41] M. Cotte, J. Susini, V. A. Sole, Y. Taniguchi, J. Chillida, E. Checroun, P. Walter, *Journal of Analytical Atomic Spectrometry* **2008** ; *23* , 820

[42] M. Cotte, E. Checroun, J. Susini, P. Walter, *Applied Physics A - Materials Science & Processing* **2007** ; *89* , 841.

[43] L. Rampazzi, A. Pozzi, A. Sansonetti, L. Toniolo, B. Giussani, *Cement and Concrete Research* **2006** ; *36* , 1108.

[44] L. Csefalvayova, M. Pelikan, I. K. Cigic, J. Kolar, M. Strlic, *Talanta* **2010** ; *82* , 1784.

[45] C. Miguel, J. A. Lopes, M. Clarke, M. J. Melo, *Chemometrics and Intelligent Laboratory Systems* **2012** ; *119* , 32.

[46] J. J. Boon, F. Hoogland, K. Keune, in *34th Annual Meeting of the AIC of Historic & Artistic Works Providence*, (Eds: H. M. Parkin), Rhode Island, **2006**, p. 16.

[47] Python Software Foundation, Python 3.2, http://www.python.org.

[48] T. E. Oliphant, *Computing in Science & Engineering* **2007** ; *9* , 10.

[49] E. Jones, T. Oliphant, P. Peterson and others, SciPy: Open Source Scientific Tools for Python, **2001-**, http://www.scipy.org/.

[50] J. D. Hunter, *Computing in Science & Engineering* **2007** ; *9* , 90.

[51] J. Romero-Pastor, C. Cardell, E. Manzano, A. Yebra-Rodriguez, N. Navas, *Journal of Raman Spectroscopy* **2011** ; *42* , 2137.

[52] S. A. Centeno, M. I. Guzman, A. Yamazaki-Kleps, C. O. Della Vedova, *Journal of the American Institute for Conservation* **2004** ; *43* , 139.

[53] P. Martinetto, M. Anne, E. Dooryhee, P. Walter, G. Tsoucaris, *Acta Crystallographica Section C - Crystal Structure Communications* **2002** ; *58* , 82.

[54] http://rruff.geo.arizona.edu/AMS/minerals/Cerussite.

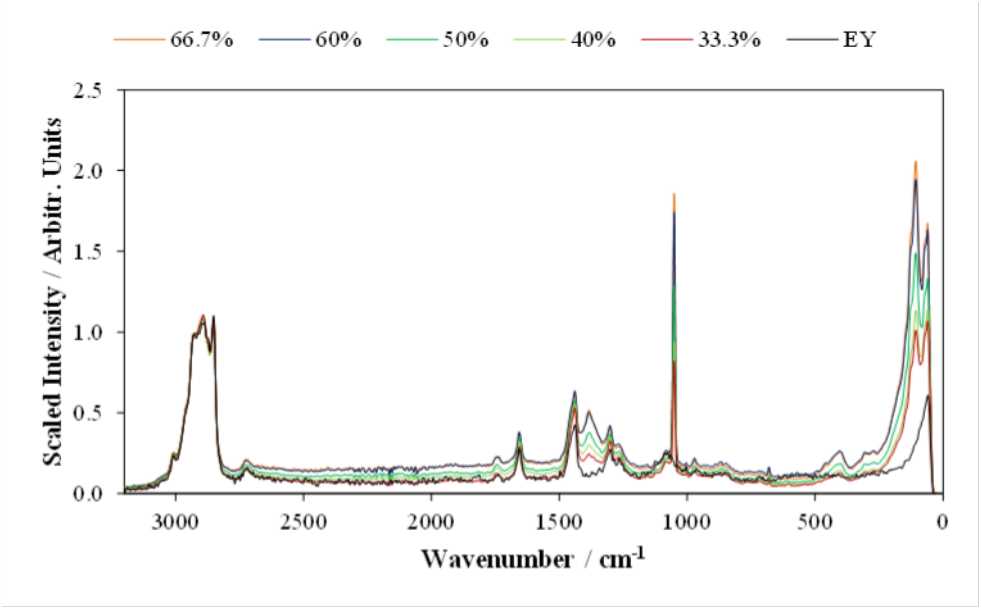
66.7%
60%
50%
40%
33.3%
EY
Scaled Intensity / Arbitr. Units
2.5
2.0
1.5
1.0
0.5
0.0
3000
2500
2000
1500
1000
500
0
Wavenumber / cm-1

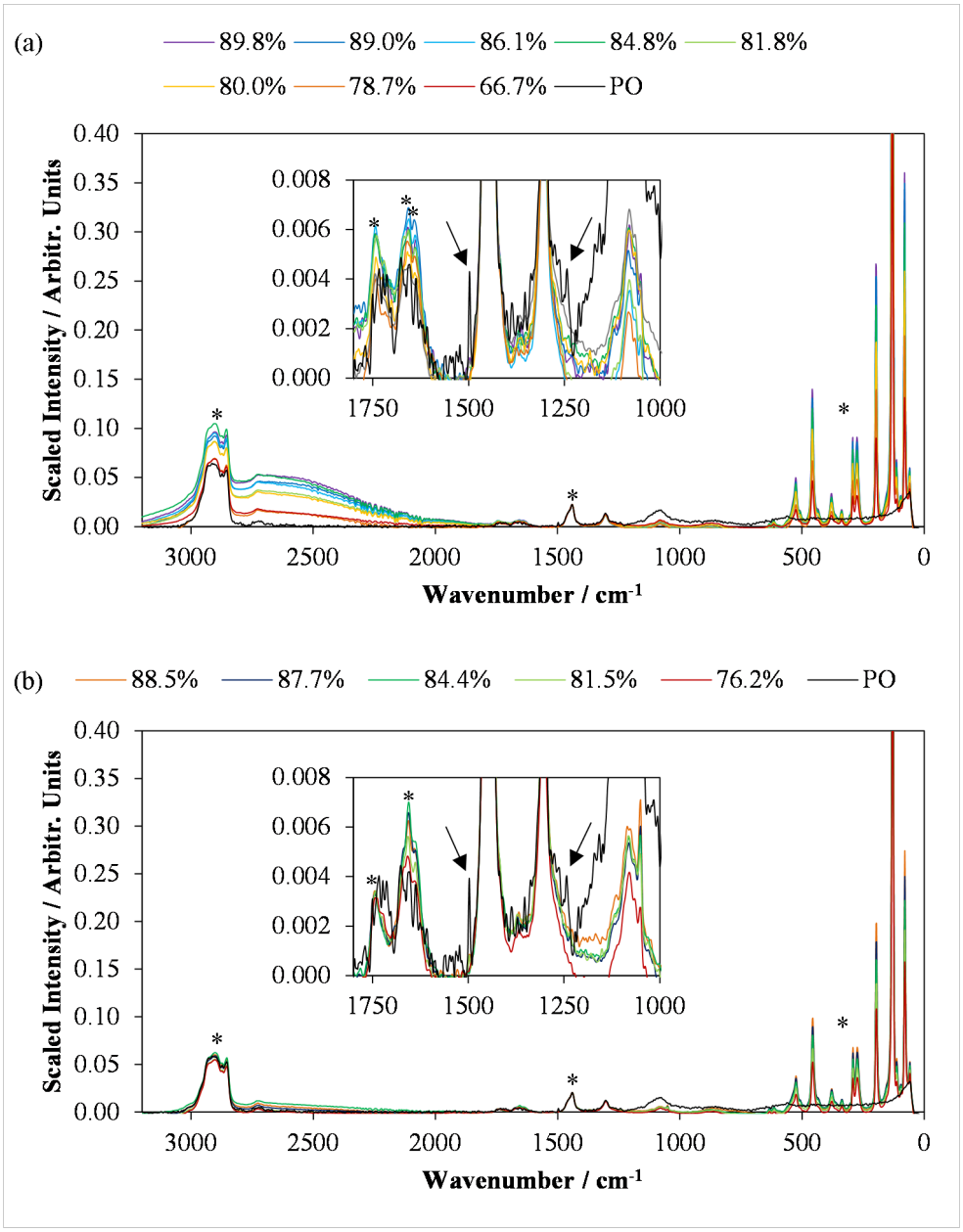
(a)
89.8%
89.0%
86.1%
84.8%
81.8%
80.0%
78.7%
66.7%
PO
Scaled Intensity / Arbitr. Units
Wavenumber / cm-1
(b)
88.5%
87.7%
84.4%
81.5%
76.2%
PO
Scaled Intensity / Arbitr. Units
Wavenumber / cm-1

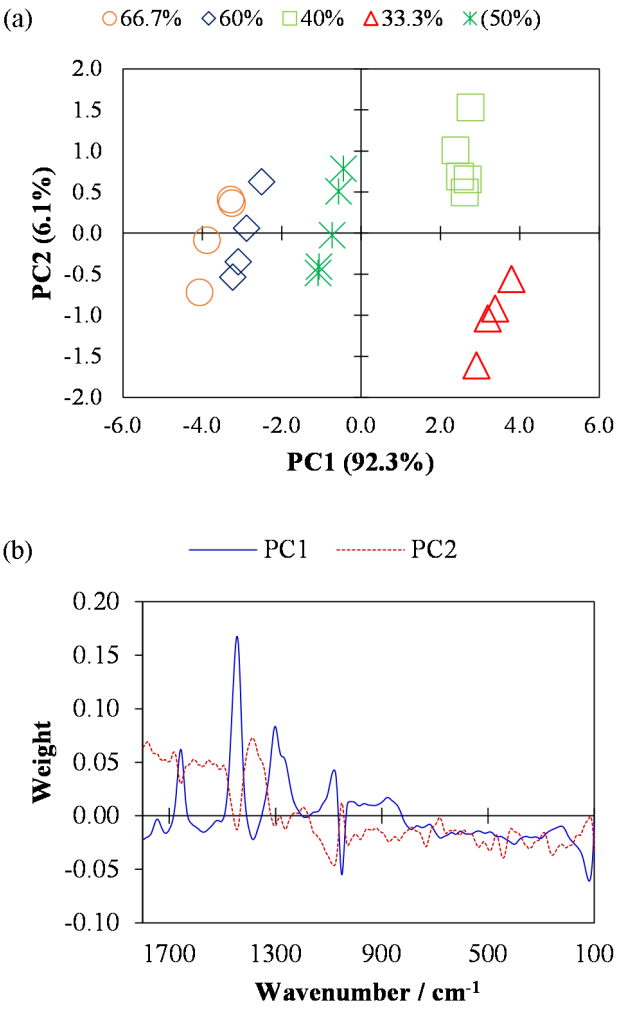
(a)
66.7%
60%
40%
33.3%
(50%)
2.0
1.5
1.0
0.5
0.0
-0.5
-1.0
-1.5
-2.0
PC2 (6.1%)
-6.0
-4.0
-2.0
0.0
2.0
4.0
6.0
PC1 (92.3%)
(b)
PC1
PC2
0.20
0.15
0.10
0.05
0.00
-0.05
-0.10
Weight
1700
1300
900
500
100
Wavenumber / cm-1

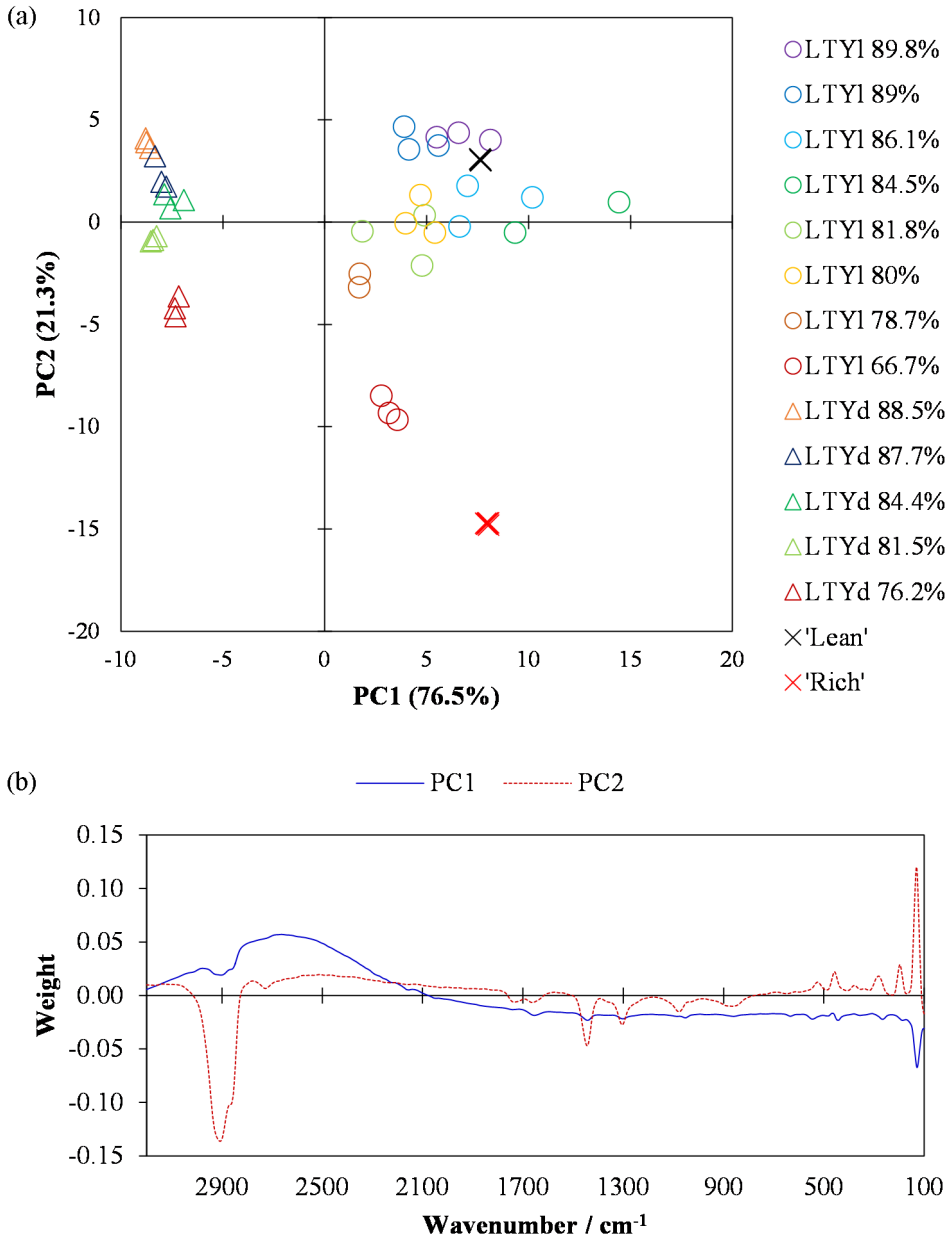
(a)
10
5
0
-5
-10
-15
-20
-10
-5
0
5
10
15
20
PC2 (21.3%)
PC1 (76.5%)
LTYl 89.8%
LTYl 89%
LTYl 86.1%
LTYl 84.5%
LTYl 81.8%
LTYl 80%
LTYl 78.7%
LTYl 66.7%
LTYd 88.5%
LTYd 87.7%
LTYd 84.4%
LTYd 81.5%
LTYd 76.2%
'Lean'
'Rich'
(b)
PC1
PC2
0.15
0.10
0.05
0.00
-0.05
-0.10
-0.15
Weight
2900
2500
2100
1700
1300
900
500
100
Wavenumber / cm-1